

Primljen / Received: 18.10.2021.

Ispravljen / Corrected: 26.4.2022.

Prihvaćen / Accepted: 30.5.2022.

Dostupno online / Available online: 10.9.2022.

## Mechanical and radiation attenuation properties of conventional and heavy concrete with diverse aggregate and water/cement ratios

### Authors:



<sup>1</sup>Assoc.Prof. **Ilker Ustabas**  
[ilker.ustabas@erdogan.edu.tr](mailto:ilker.ustabas@erdogan.edu.tr)



<sup>2</sup>**Mustafa Demirci**, MCE  
[mustafa.demirci@erdogan.edu.tr](mailto:mustafa.demirci@erdogan.edu.tr)



<sup>3</sup>Prof. **Hasan Baltas**  
[hasan.baltas@erdogan.edu.tr](mailto:hasan.baltas@erdogan.edu.tr)



<sup>4</sup>Assoc.Prof. **Yilmaz Demir**  
[yilmaz.demir@erdogan.edu.tr](mailto:yilmaz.demir@erdogan.edu.tr)



<sup>5</sup>Prof. **Sakir Erdogan**  
[shake@ktu.edu.tr](mailto:shake@ktu.edu.tr)



<sup>1</sup>**Zafer Kurt**, MCE  
[zafer.kurt@erdogan.edu.tr](mailto:zafer.kurt@erdogan.edu.tr)  
Corresponding author



<sup>1</sup>**Talip Cakmak**, MCE  
[talip.cakmak@erdogan.edu.tr](mailto:talip.cakmak@erdogan.edu.tr)

<sup>1</sup> Recep Tayyip Erdogan University, Rize, Turkey  
Engineering and Arts Faculty  
Department of Civil Engineering

<sup>2</sup> Recep Tayyip Erdogan University, Rize, Turkey  
Technical Vocational School Construction  
Technology Program

<sup>3</sup> Recep Tayyip Erdogan University, Rize, Turkey  
Engineering and Arts Faculty  
Science and Literature Faculty, Department of Physics

<sup>4</sup> Recep Tayyip Erdogan University, Rize, Turkey  
Engineering and Arts Faculty  
Department of Geology Engineering

<sup>5</sup> Karadeniz Technical University, Trabzon, Turkey  
Engineering and Arts Faculty

Research Paper

**Ilker Ustabas, Mustafa Demirci, Hasan Baltas, Yilmaz Demir, Sakir Erdogan, Zafer Kurt, Talip Cakmak**

### Mechanical and radiation attenuation properties of conventional and heavy concrete with diverse aggregate and water/cement ratios

This paper presents the results of comprehensive laboratory work conducted for investigating the mechanical and radiation attenuation characteristics of heavyweight concrete produced with pyrite, chromium, and magnetite aggregates and normal weight concretes produced with three different water/ cement (w/c) ratios. Various experiments were conducted to determine the compressive strengths, ultrasound transmission velocities, experimental elasticity modules, and mass attenuation coefficients of these concretes. Heavy and normal weight concretes exhibited similar behaviour in terms of compressive strength and elasticity modules. In heavyweight concretes, with increased w/c ratios (by keeping the amount of water constant and decreasing the amount of cement), the corresponding density increased due to the increase in the amount of high-density aggregates rather than cement in the composition of concrete. Thus, heavyweight concretes produced with a high w/c ratio and low strength can absorb more X-rays. Mass attenuation coefficients converge in heavy and normal weight concretes with different densities at high energy levels.

#### Key words:

heavyweight concrete, elasticity modules, magnetite aggregate, mass attenuation coefficient

Prethodno priopćenje

**Ilker Ustabas, Mustafa Demirci, Hasan Baltas, Yilmaz Demir, Sakir Erdogan, Zafer Kurt, Talip Cakmak**

### Ispitivanje mehaničkih svojstava i svojstava smanjenja zračenja običnog i teškog betona s različitim agregatima i vodocementnim omjerima

Ovim istraživanjem predstavljaju se rezultati sveobuhvatnog laboratorijskog rada kojemu je cilj ispitati mehanička svojstva i svojstva smanjenja zračenja teških betona u kojima se kao agregat koristio pirit, krom i magnetit te betona normalne težine koji su se proizveli s tri različita vodocementna omjera ( $v/c = 0,4/0,5/0,6$ ). U laboratoriju su provedena ispitivanja tlačne čvrstoće, brzine prolaska ultrazvuka, eksperimentalni modul elastičnosti te koeficijenta prigušenja mase tih betona. Na temelju provedenih ispitivanja utvrđeno je da betoni normalne težine i teški betoni imaju slično ponašanje u smislu tlačne čvrstoće i modula elastičnosti. U slučaju teških betona (njihovi v/c omjeri povećani su uslijed konstantne količine vode te smanjene količine cementa), gustoća se povećava zbog povećanja količine agregata veće gustoće u odnosu na cement u sastavu betona. To je razlog zašto teški betoni koji su proizvedeni s većim v/c omjerom te koji su manje čvrstoće mogu apsorbirati više rendgenskih zraka. Koeficijenti prigušenja mase konvergiraju pri visokim energetske razinama kod teških i normalnih betona različitih gustoća.

#### Ključne riječi:

teški beton, modul elastičnosti, agregat magnetita, koeficijent prigušenja mase

### 1. Introduction

The technological developments during the last two decades have introduced radiation-emitting devices that are in close proximity to people. Thus, materials with high radiation attenuation coefficients must be used to prevent damage to the environment from radiation-emitting devices. Concrete is a cheap, durable, and protective material commonly used against radioactive radiation [1, 2]. It can be used as a protective barrier, especially in places such as nuclear power plants and radiation units of hospitals. High-density concretes provide more protection against radiation. Using high-density aggregates increases the density of concrete and reduces its thickness while absorbing the same dose of radiation [3, 4]. According to TS EN 206, concretes with a unit weight above 2,600 kg/m<sup>3</sup> are categorised as heavyweight concrete (HWC) [5], which absorb more radiation than conventional concrete (CC). Rocks with high-density minerals are the most preferred for heavy concrete aggregate [1, 2, 6]. Absorption properties of concretes made by barite, magnetite, serpentine, and hematite aggregates are explored in the literature [2, 4, 6–11]. The critical challenge in the mixtures of HWCs using aggregates with high unit weight is determining the water/cement (w/c) ratio. Heavy density aggregates may cause segregation in concretes with high consistency. Saidani et al. [2] designed heavyweight concrete with 10–12 cm slumps using barite aggregate. Lotfi-Omran [12] designed heavy concrete with 4–8 cm slumps using magnetite aggregates. Aiming to design HWCs with high slump values, 18 cm slumps were used in this study to produce heavy and normal concretes. Topcu [13] reported that the w/c ratio is important in reducing the radioactive permeability and the shrinkage cracks in concrete. Prochon et al. [14] reported that unlike the w/c ratio of granite-based concrete, aggregate/cement types are important in absorbing radiation. Bellum et al. [17] compared their modulus of elasticity with certain standards, and the modulus of elasticity that researchers found was between 12.904 GPa and 31.107 GPa. Aggregates and cementitious binders used in concrete affect the strength and elasticity of concrete [16–21]. Elasticity modulus is a key property in improving the mechanical properties of concrete [22–24]. However, other studies found a key correlation between the strength of concrete and its elastic modulus more than its aggregate type [17, 25] and its radiation absorption characteristics. Although there are radiation absorption-based works in the literature, studies on radiation absorption properties of heavy aggregate concretes are limited. The radiation absorption properties of heavy concrete using chromium and pyrite aggregate (obtained from chromium and pyrite rocks) are discussed for the first time in this study. Three w/c ratios (0.4, 0.5, and 0.6) were selected to determine the influence of the w/c ratio on the HWCs radiation attenuation. This study aims to explore the influence of diverse heavy aggregates (pyrite, chromium, and magnetite) on the radiation absorption behaviour of concrete.

Several experiments to determine the compressive strength, density, ultrasound transmission velocity, surface hardness, and elastic modulus were performed on conventional and HWCs produced with different aggregate types (with normal, pyrite, chromium, and magnetite). The effect of normal and heavy aggregates on the elastic modulus of concrete was investigated. Thus, the influence of heavy aggregates on concrete’s strength properties was explored. Moreover, the radiation mass attenuation constants of the produced CCs and HWCs were evaluated.

### 2. Materials and methods

#### 2.1. Materials

CEM I 42.5 R type cement was employed in the produced concrete. Rocks containing pyrite, chromium, and magnetite aggregates were collected from the districts of Kop (Bayburt), Murgul (Artvin), and Araklı (Trabzon) in Turkey. They were ground in a jaw crusher. The crushed material was sieved in the jaw crusher, and the coarse and fine aggregates were separated. With these aggregates, pyrite aggregate HWC (HWC-P) with a w/c ratio of 0.4–0.6, chromium aggregate HWC (HWC-C), magnetite-weight aggregate HWC (HWC-M), and CC were produced. X-ray Fluorescence (XRF) analysis of the parts taken from these CCs and HWCs was performed on the powdered material. Table 1 lists the XRF analysis results of the concrete. The amount of MgO in HWC-C was measured between 15 % and 20 %. This is because the MgO content of the chromite aggregate used in HWC-C is 23 %. The amount of FeS in the HWC-P was measured as the amounts of Fe<sub>2</sub>O<sub>3</sub> and SO<sub>3</sub>. The high SO<sub>3</sub> amount in HWC-P is due to the sulfur (S) in FeS. Excess MgO and SO<sub>3</sub> in the cement causes expansion and setting problems. MgO is present in the chromite aggregate in this study.

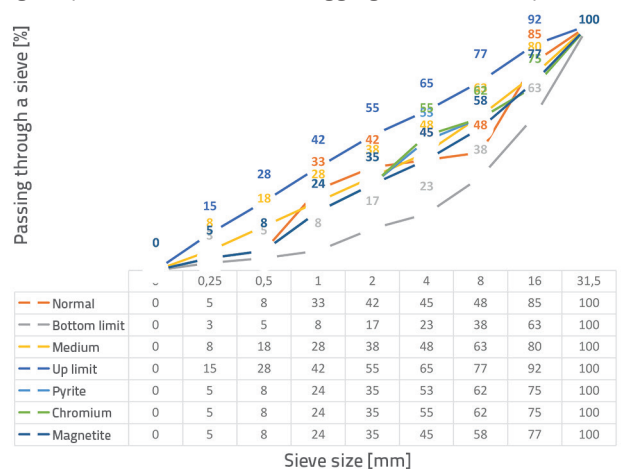


Figure 1. The sieve analysis results of aggregates used in CC, HWC-P, HWC-C, and HWC-M

In Figure 1, the particle size distribution curves according to TS 802 and the granulometry curves of the aggregates used

**Table 1. Chemical composition of concretes having a w/c ratio of 0.4, 0.5, and 0.6 (considered as %)**

	CC			HWC-P			HWC-C			HWC-M		
	0.40	0.50	0.60	0.40	0.50	0.60	0.40	0.50	0.60	0.40	0.50	0.60
LOI	4.8	4.3	3	6.04	6.14	6.64	7.5	6.9	6.5	6.9	6.5	6
Al <sub>2</sub> O <sub>3</sub>	11	11.3	12	2.58	3.08	3.24	6.89	7.42	7.26	3.37	4.07	3.23
BaO	0.04	0.05	0.04	0.029	0.04	0.03	0	0	0	0.03	0.04	0.03
CaO	11.2	9.72	6.79	7.47	6.83	4.91	11.7	6.67	4.85	23.4	22	21.8
Cr <sub>2</sub> O <sub>3</sub>	0.009	0.009	0.01	0.055	0.024	0.063	19.3	25.9	26.7	0.023	0.023	0.045
Fe <sub>2</sub> O <sub>3</sub>	3.61	3.58	3.78	7.79	8.16	8.36	12.4	13.7	13.3	24.7	22.7	28.5
K <sub>2</sub> O	0.89	1.06	0.92	0.75	0.66	0.74	0.5	0.37	0.31	0.46	0.61	0.38
MgO	1	0.97	1.11	0.67	0.48	0.48	15.2	17.5	20	1.87	1.76	2.19
MnO	0.1	0.09	0.1	0.06	0.04	0.04	0.21	0.17	0.15	0.84	0.93	0.93
Na <sub>2</sub> O	3.89	3.84	4.33	0.43	0.42	0.36	0.31	0.19	0.14	0.46	0.8	0.42
P <sub>2</sub> O <sub>5</sub>	0.077	0.078	0.077	0.045	0.037	0.029	0.043	0.02	0.015	0.142	0.138	0.193
SO <sub>3</sub>	0.5	0.45	0.38	11.05	12.64	13.45	0.63	0.4	0.3	0.72	0.94	0.42
SiO <sub>2</sub>	61.8	63.3	66.2	63.2	61.6	61.3	22.8	19.3	19.1	35.9	38.3	34.9
TiO <sub>2</sub>	0.32	0.33	0.35	0.1	0.09	0.09	0.15	0.15	0.14	0.09	0.1	0.08
V <sub>2</sub> O <sub>5</sub>	0.015	0.014	0.011	0.019	0.016	0.012	0.056	0.069	0.066	0.014	0.014	0.012
ZnO	0.01	0.017	0.013	0.038	0.032	0.026	0.089	0.045	0.039	0.361	>1.000	0.456
ZrO <sub>2</sub>	0.03	0.03	0.03	0.02	0.02	0.02	0	0	0	0.02	0	0.01
Total	99.29	99.17	99.16	100.34	100.30	99.79	98.8	99.6	100.39	99.33	100.14	99.58

CC: Conventional concrete; HWC-P: Heavyweight concrete with pyrite; HWC-C: Heavyweight concrete with chromium; HWC-M: Heavyweight concrete with magnetite

**Table 2. Specific gravity and water absorption values of aggregates**

	Normal aggregates			Magnetite			Pyrite			Chromium		
	Coarse 1	Coarse 2	Fine	Coarse 1	Coarse 2	Fine	Coarse 1	Coarse 2	Fine	Coarse 1	Coarse 2	Fine
SG	2.61	2.64	2.51	3.30	3.36	3.07	4.52	4.74	4.31	3.40	3.18	3.07
WA [%]	1.39	0.85	3.43	2.43	0.46	10.3	1.47	0.60	3.62	0.92	0.64	6.11

Coarse 1: the thickest aggregate; Coarse 2: medium-sized aggregate; Fine: the thinnest aggregate; SG - Specific gravity; WA - Water absorption

in CC and HWC are shown. The specific weights and water absorption values of the aggregates used in concrete are summarised in Table 2.

## 2.2. Mix design

Cylindrical (diameter: 100 mm, height: 200 mm) and cubic (150×150×150 mm) concrete samples were formed, as shown in Figure 2.

To explore the mechanical and radiation characteristics of heavy concretes, concretes with an 18 cm slump with blending rates shown in Table 3 were produced according to TS 802. Concretes were manufactured by employing three diverse heavy aggregates and one normal aggregate with three different w/c ratios (0.4, 0.5, and 0.6). The amount of water was kept equal in all groups so that the concrete settling was equal. In all concretes, 190 kg of water was

added to 1 m<sup>3</sup> of concrete. The concretes were mixed with a pan-type mixer in a volume of 16 litres at one time and filled with 25 skewers in each layer.

**Figure 2. Making cylindrical and cubic concrete samples**

Table 3. Concrete blending rates

Concrete types	w/c ratio	Cement [kg]	Water [kg]	Aggregates [kg]			Chemical addition [kg]	Total [kg]	Slump [mm]
				Coarse 1	Coarse 2	Fine			
CC	0.40	475	190	427	511	642	14.25	2259.25	185
	0.50	380	190	452	540	679	7.60	2248.60	195
	0.60	317	190	468	560	703	3.17	2241.17	210
HWC-M	0.40	475	190	525	619	711	14.25	2534.25	190
	0.50	380	190	555	655	751	7.60	2538.6	195
	0.60	317	190	575	678	779	3.17	2542.17	200
HWC-P	0.40	475	190	750	850	886	14.25	3165.25	150
	0.50	380	190	793	899	937	7.60	3206.6	165
	0.60	317	190	821	931	971	3.17	3233.17	160
HWC-C	0.40	475	190	538	616	726	14.25	2559.25	175
	0.50	380	190	569	651	767	7.60	2564.6	175
	0.60	317	190	589	654	795	3.17	2568.17	165

### 2.3. Experimental techniques

The uniaxial compressive strengths of the cubic and 90-day cured concretes were measured using a UTEST mechanical press (Figure 3) according to the standard TS EN 12350-3. The ultrasound transmission velocity of the concretes and their surface hardness were measured using an ultrasonic pulse velocity tester (Proceq) and a Schmidt test hammer. The lateral and axial length changes of concretes according to the applied compressive stress ( $\sigma$ ) were measured. Elastic modulus was experimentally measured from the stress versus strain ( $\epsilon$ ) plot from the press. The tangent, secant (static), and chord (beam) moduli of elasticity of concretes were calculated. The secant elastic modulus was computed from the slope of the line joining the origin to the value corresponding to 40 % of the ultimate compressive strength on the  $\sigma$ - $\epsilon$  curve. The tangent elastic modulus was calculated from the hill of the tangent at  $0.4x f_{ck}$  to the  $\sigma$ - $\epsilon$  curve. The chord (beam) elastic modulus was computed from the hill of the line combining the  $50 \times 10^{-6}$  strain value of the  $\sigma$ - $\epsilon$  curve and 40 % of the compressive strength.

Three test samples were used for each group of concretes in the study. Before applying the compressive strength, ultrasound transmission velocity and surface hardness values were measured using 15 cm<sup>3</sup> concrete samples. Then, the compressive strengths of each group of concrete samples were measured. For the compressive strength, ultrasound transmission rate, and surface hardness values, 36 cubic concrete samples with a length of 15 cm were used. In addition, 36 cylindrical concrete samples were used

to measure elastic modulus. The experimental methodology is shown in Figure 4.

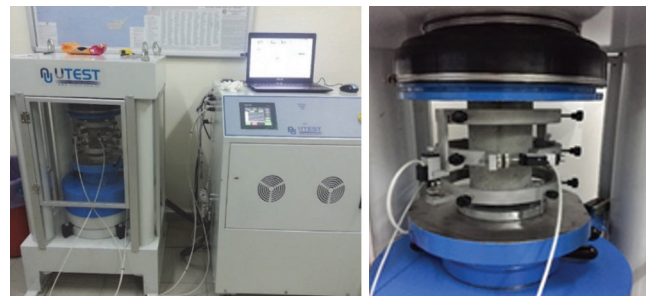


Figure 3. Concrete press and compressometer used for measuring the modulus of elasticity

The concretes cut from the concrete samples produced, were ground in a ring grinder and turned into powder. To evaporate the remaining water, the samples were dried in an oven at 105 °C for 1 d. For the analysis, 4-g samples were prepared by pressing

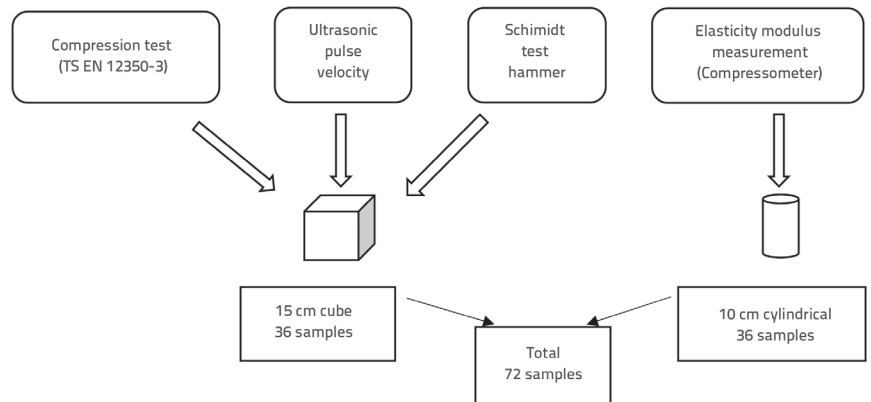


Figure 4. Test program table

them with a hydraulic press under 7 tons of pressure for 20 seconds with a diameter of 40 mm. To determine the mass attenuation coefficients of the materials used, experiments were carried out by employing a semiconductor gamma detector (ORTEC brand GEM25P4-76 model HPGe) with a 25 % relative efficiency and 1.33 MeV discrimination power of 1.70 keV. A narrow beam geometry shown in Figure 5 was created for experimental studies.

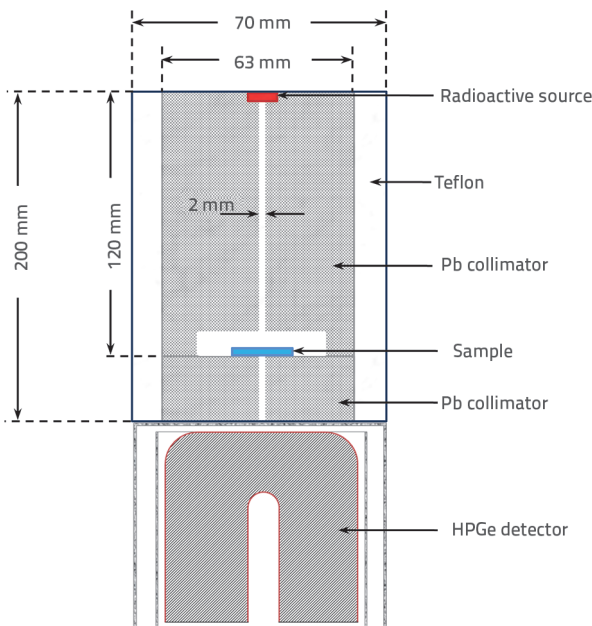


Figure 5. Experiment geometry used in the measurement of mass attenuation coefficients [26]

To abolish the geometric influences affecting CC during sample/source change, independent windows are left in test geometry. Mass attenuation coefficients were measured for 5 different energy values in the range of 59.5, 122, 661, and 1332 keV. The mass attenuation coefficients for the materials used were computed by using the Lambert-Beer law

$$I = I_0 e^{-\frac{\mu}{\rho} d} \tag{1}$$

where  $\mu/\rho$  represents the mass attenuation coefficient for the materials used ( $\text{cm}^2/\text{g}$ ), and  $d$  stands for the surface density of the samples ( $\text{g}/\text{cm}^2$ ),  $I_0$  and  $I$  are the intensities of beams emitted from the source at a solid angle in narrow beam geometry and that passing the sample and reaching the detector, respectively. To measure the intensity ( $I_0$ ) of the beam emitted from the source and reaching the detector, the measurement process was carried out without placing the absorbent sample between the source and detector.

Then, the intensity ( $I$ ) of the beam passing the sample and reaching the detector was determined by placing the absorbent sample in between. Each measurement process was repeated three times for 5,000 s.

### 2.4. Instrumental techniques

The ultrasound velocity is related to the strength of the concrete. The device sends and receives signals from receiver and transmitter sensors to the wave's medium and measures the rate of diffusion in concrete. Tests for pressure in accordance with 100x200 mm cylindrical samples used were performed to measure the transmission speed. Low-frequency signals produced by the device were transmitted from inside the sample to the opposite side, which were detected by transducers at the ends, and signals were transmitted through the sample. The transition times were also determined. The transit time is related to the density and quality of the sample. The probes of the ultrasound device, on which samples are cleaned and gel is applied, will lie on the parallel plane coinciding with the two opposite surfaces of the sample. The sound transmission velocity ( $V$ ) was calculated by the equation given below, [28]:

$$v = \frac{L}{t} \tag{2}$$

where:

- $V$  - the ultrasound speed [m/s]
- $L$  - the transition length [m]
- $T$  - the transition time [s].

### 3. Result and discussion

Table 4 shows the fresh and hardened concrete unit volume weights, compressive strength, hardened unit volume weights, surface hardness, and ultrasound transmission velocities of the CC, HWC-P, HWC-C, and HWC-M measured with the Schmidt test hammer. The values in Table 4 were averaged from three concrete samples.

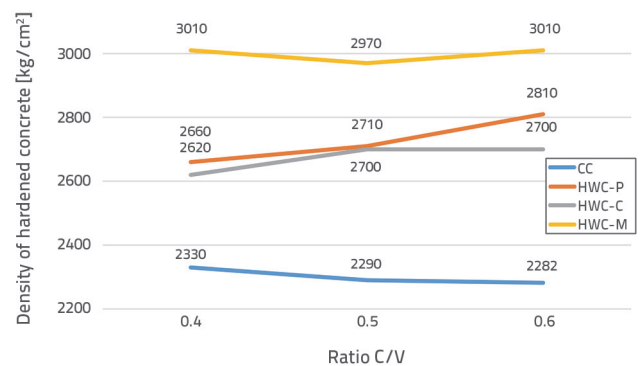


Figure 6. Hardened concrete densities in conventional and heavy concretes with pyrite, chrome, and magnetite aggregates

Figure 6 shows the hardened concrete densities. In the samples, the water amount is kept constant while the cement amount is increased, thereby decreasing the w/c ratios. More cement is included in concrete composition where the w/c ratio is reduced in CC. The increase in w/c ratio caused a drop in the density of the concrete due to the decrease in the amount of cement added to

**Table 4. Density, compressive strength, surface hardness values, and ultrasound transmission velocities of CC, HWC-P, HWC-C, HWC-M made with diverse water-cement ratios**

Concrete types	w/c ratio	Fresh concrete density [kg/m <sup>3</sup> ]	Hardened concrete density [kg/m <sup>3</sup> ]	15 cm cube aamples compressive strength [N/mm <sup>2</sup> ]	Schmidt hammer surface hardness values	15 cm cube samples ultrasound transmission velocities [km/s]
CC	0.4	2297	2330	48.3	31	4.73
	0.5	2288	2290	33.6	29	4.49
	0.6	2282	2300	28.6	27	4.59
HWC-P	0.4	2601	2660	50.0	38	4.63
	0.5	2610	2710	44.5	34	4.46
	0.6	2615	2810	31.0	27	4.39
HWC-C	0.4	2604	2620	35.6	35	4.53
	0.5	2613	2700	24.8	25	4.57
	0.6	2619	2700	19.5	22	4.20
HWC-M	0.4	3213	3010	42.1	30	4.53
	0.5	3257	2970	29.3	28	4.62
	0.6	3286	3010	21.6	24	4.66

the CC because the density of cement is higher than the density of the aggregate. Among the samples considered, CC has the lowest density at a 0.6 w/c ratio. The opposite was observed in heavy concretes. The concrete density increases with the w/c ratio. As the w/c ratio increases in HWCs, the amount of cement added to the concrete decreases while the amount of aggregate increases. This is because the density of the aggregate is higher compared to that of the cement. Saidani et al. [2] used a limestone aggregate instead of a coarse aggregate with barite (density = 4.06 g/cm<sup>3</sup>) in concretes with a 0.5 w/c ratio; the samples had hardened concrete densities in the range of 32 to 2.48 g/cm<sup>3</sup>. In this study, since the fine aggregate used in HWCs was heavy, the hardened concrete density in concretes with a w/c ratio of 0.5 was between 2.7 and 2.97 g/cm<sup>3</sup>. Thus, HWCs were produced with high-density aggregates exceeding 2.6 g/cm<sup>3</sup>. According to Saidani et al. [2], by using low-density, fine aggregates, the hardened concrete densities will remain below 2.6 g/cm<sup>3</sup>. Sharifi et al. [6] produced concretes with a density of 3.35, 2.6, and 5.1 g/cm<sup>3</sup> using barite, serpentine, and magnetite to measure the mass attenuation coefficients and measured the radiation attenuation properties of these concretes. Oto et al. [4] produced 100 % magnetite aggregate concretes with a density of 2.78 g/cm<sup>3</sup> and HWCs with a ratio of 0.5 w/c. The density of

the magnetite aggregate concrete with a 0.5 w/c ratio produced in this study was measured as 2.97 g/cm<sup>3</sup>. Lotfi-Omran et al. [12] revealed that as the w/c ratio decreases, the density of the heavy concrete produced with magnetite decreases. Since the density of cement in heavy concrete is lower than that of the magnetite aggregate, increasing the amount of cement and decreasing the w/c ratio decreases the density of heavy concrete. The results found in this study were similar to those by Lotfi-Omran et al. [12] for pyrite, chromium, and magnetite aggregates.

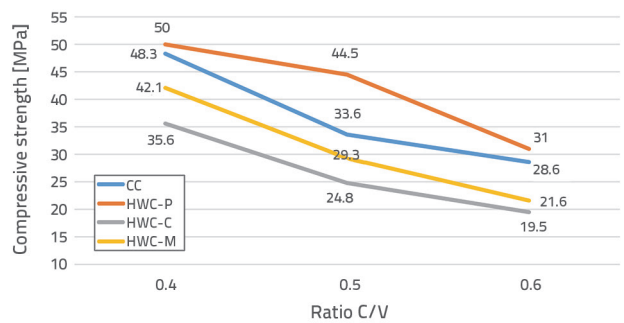


**Figure 7. Compressive strengths measured in conventional and heavyweight concretes**

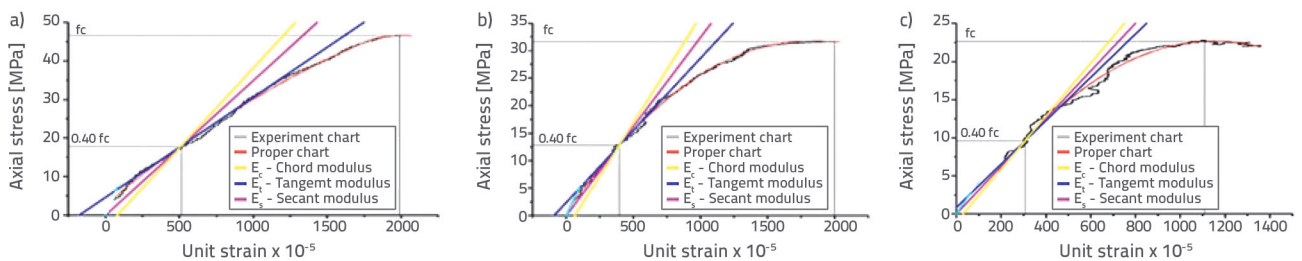


**Figure 8. Stress-strain graph of 90-day cured CCs with a w/c ratio of w/c ratios: a) 0.40; b) 0.5; c) 0.6**

Table 5. Elasticity moduli of CC, HWC-C, HWC-P and HWC-M

Concrete types	w/c ratio	Compressive strength $f_c$ [MPa]	Elasticity modulus [GPa]		
			Tangent	Secant	Chord
CC	0.4	46.50	31.630	36.214	36.471
	0.5	31.70	34.750	34.270	39.625
	0.6	22.80	32.350	26.824	31.448
HWC-C	0.4	36.20	30.920	35.692	30.919
	0.5	31.80	31.810	37.913	31.809
	0.6	22.90	29.220	26.941	29.219
HWC-P	0.4	53.00	32.950	38.545	32.949
	0.5	43.80	36.230	29.200	36.229
	0.6	33.50	25.260	28.511	25.590
HWC-M	0.4	40.50	38.540	36.400	36.000
	0.5	27.00	29.310	32.241	35.000
	0.6	18.00	14.260	21.818	25.714

Figure 7 shows the compressive strengths measured for CC, HWC-P, HWC-C, and HWC-M 15 cm cubic specimens. As the w/c ratio increases, the compressive strength of the concretes decreases. HWC-P and HWC-C have the highest and lowest compressive strengths, respectively. Saidani et al. [2] obtained concrete strengths with a compressive strength of 28 to 40 MPa in normal and barite aggregate concretes with a 0.5 w/c. Compressive strengths between 25 and 45 MPa were found in the concretes in this study.

The compressive strength of HWC-M was similar to that of concretes with 100 % barite aggregate in Saidi et al. [2]. Also, the use of fine pyrite aggregates increased the concrete strength. In this study, decreasing w/c ratios results in increasing the concrete strength for denser structures. In Table 2, the pressure resistance increases in concretes with decreasing w/c ratios. In high-strength concrete, the Schmidt test hammer value and ultrasound transmission speed increase. Compression and unit length changes in 100 and 200 mm cylindrical samples of CC, HWC-P, HWC-C, and HWC-M 100/200 (mm/mm) diameter/length ratio are shown in Figure 8. Secant, tangent, and chord elasticity moduli were calculated from the stress-strain ( $\sigma$ - $\epsilon$ ) graphs shown in Figure 8. Figure 8 shows the stress-strain graph obtained from CCs with 0.40 (a),

0.5 (b), and 0.6 (c) w/c ratios. The calculated elasticity moduli are listed in Table 5.

As shown in Table 5, the elastic moduli range between 26.824 and 42.350 GPa. The elastic modulus increases with increasing concrete strength. However, variances are observed in the stress and elastic moduli measured using the mechanical press (Table 5).

Figures 9 to 11 show the stress-strain curves of HWCs. As w/c ratios increased in CC, HWC-P, HWC-C, and HWC-M, the compressive strength and elastic moduli of concretes also increased. According to the type of aggregate, a significant difference was not observed between CC and HWCs. Bellum et al. [17] calculated the static elastic moduli between 13.362 and 20.196 GPa in concretes with a compressive strength of 15.46 MPa and 38.24 MPa. Bilir [25] compared the elastic moduli in concretes with high compressive strength in the range of 70–100 MPa with those recommended by the standards, and the static elastic moduli between 28 and 43 GPa.

Yildirim and Sengul [17] found an elastic modulus between 15 and 50 GPa in normal concretes, depending on the w/c ratio. The elastic moduli of concretes in this study are compatible with the results of other studies [15, 18, 19].

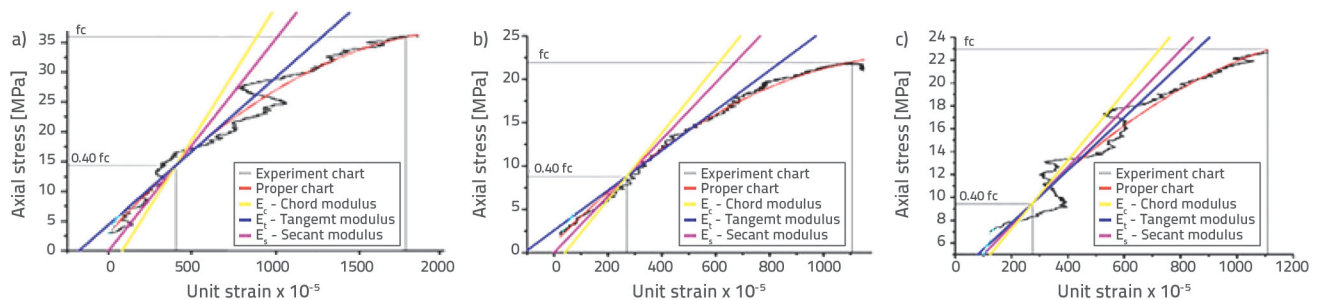


Figure 9. Stress-strain graph of 90-day cured HWC-Cs with w/c ratios: a) 0.40; b) 0.5; c) 0.6

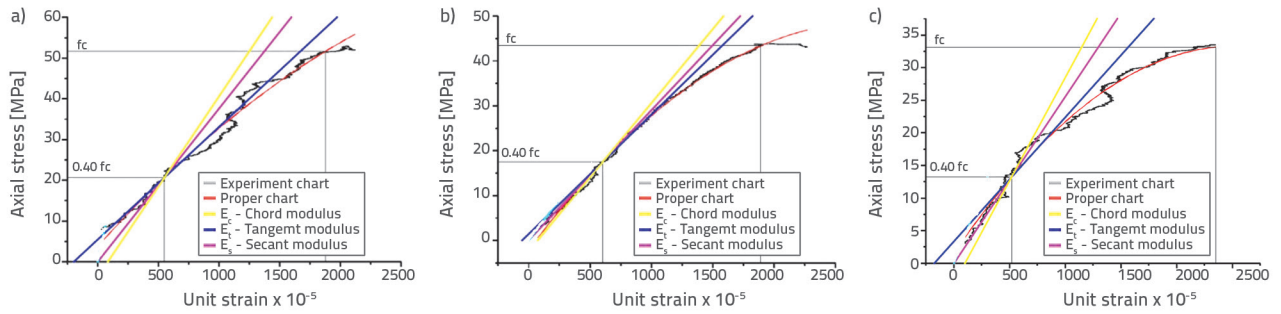


Figure 10. Stress-strain graph of 90-day cured HWC-Ps with w/c ratios: a) 0.40; b) 0.5; c) 0.6

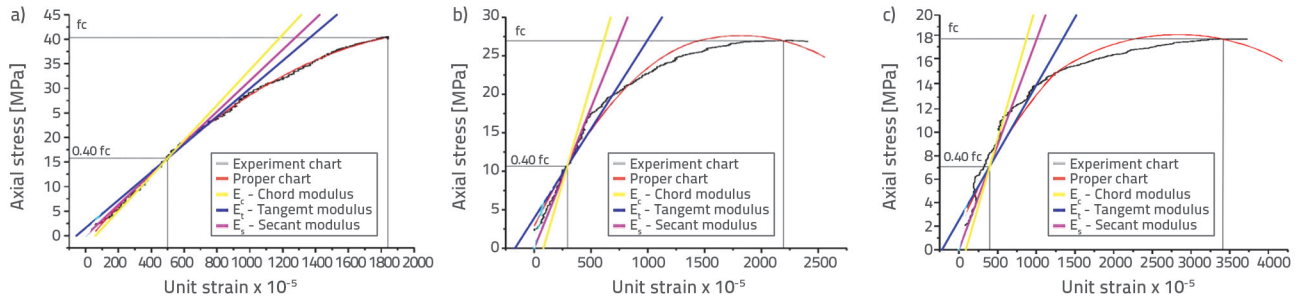


Figure 11. Stress-strain graph of 90-day cured magnetite aggregate concrete made with w/c ratios: a) 0.40; b) 0.5; c) 0.6

Yıldırım and Sengul [17] prepared concretes in diverse mixes and found the static elastic modulus between 15 and 50 GPa. Figure 11 shows the secant (static) elastic modulus measured experimentally with aggregates having normal, pyrite, chromium, and magnetite aggregates. Secant elastic moduli increase as the w/c ratio of concrete decreases. However, the increase in compressive strength due to the decrease in the w/c ratio in the concrete causes a difference in the calculation of the elastic moduli of some concretes. The elastic modulus of concrete with a 0.4 w/c ratio is less than that of the normal concrete with a 0.5 w/c ratio. The elastic modulus of magnetite concrete with a 0.4 w/c ratio is lower than with a 0.5 w/c ratio. Experimentally, the measurement of the elastic modulus of concrete is very sensitive, which can result in differences, as shown here. Elastic module of normal weight concrete according to TS 500:

$$E_{cj} = 3250\sqrt{f_{ckj}} + 14000 \tag{3}$$

According to ACI 318 M-95

$$E_c = 4700\sqrt{f_c} \tag{4}$$

It is seen that the elasticity moduli calculated from the formula suggested by TS 500 and Figure 12 are higher than those calculated using the ACI 318M-95 standard. From Figure 12, the elasticity moduli calculated experimentally in this study are close to those suggested by both standards. The elastic moduli of heavy concrete were not affected by the difference in

aggregate density and showed similar behaviour to the elastic modulus of CC.

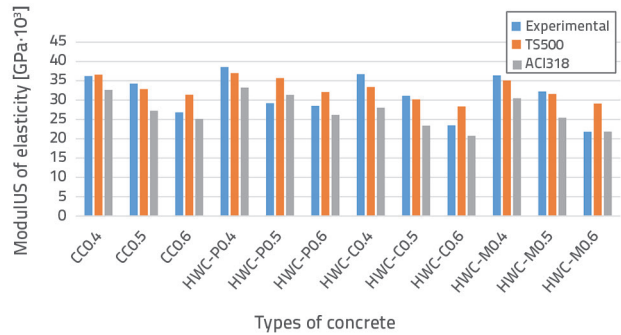


Figure 12. Secant elastic modulus of concretes

Table 6 lists the experimental and theoretical mass absorption coefficients for concrete. Figure 13 shows the mass absorption coefficients of CC at different energy levels and w/c ratios. As the w/c ratio decreases at low energy levels (59.5 and 122 keV), the density of concrete increases, and the mass absorption coefficient increases in concretes with high density. Figure 13 shows that concretes with 0.4 w/c ratios at 59.5 and 122 keV energy levels have the highest mass absorption coefficient, followed by concretes with 0.5 and 0.6 w/c ratios. Oto et al. [4] calculated mass absorption coefficients ranging from 0.7 to 0.05 at energy levels of 59.5 to 1332 keV for conventional and magnetite aggregate concretes with a density of 2.58 to 2.78 g/cm<sup>3</sup>, respectively.

Table 6. Experimental and theoretical mass attenuation coefficients

Energy level		Mass attenuation coefficients according to energy levels [cm <sup>2</sup> /g]							
		59.5 keV		122 keV		661 keV		1332 keV	
Concrete types	w/c ratio	Experimental	Theoretical	Experimental	Theoretical	Experimental	Theoretical	Experimental	Theoretical
CC	0.4	0.323 ± 0.007	0.317	0.161 ± 0.004	0.160	0.075 ± 0.001	0.077	0.052 ± 0.001	0.055
	0.5	0.320 ± 0.007	0.314	0.161 ± 0.004	0.159	0.077 ± 0.001	0.077	0.054 ± 0.001	0.055
	0.6	0.300 ± 0.007	0.304	0.159 ± 0.004	0.158	0.078 ± 0.001	0.077	0.054 ± 0.001	0.055
HWC-C	0.4	0.490 ± 0.009	0.484	0.179 ± 0.004	0.178	0.076 ± 0.001	0.076	0.052 ± 0.001	0.054
	0.5	0.513 ± 0.009	0.507	0.182 ± 0.004	0.180	0.075 ± 0.001	0.076	0.051 ± 0.001	0.054
	0.6	0.507 ± 0.009	0.500	0.181 ± 0.004	0.179	0.075 ± 0.001	0.076	0.052 ± 0.001	0.054
HWC-M	0.4	0.523 ± 0.009	0.517	0.184 ± 0.004	0.183	0.077 ± 0.001	0.077	0.053 ± 0.001	0.054
	0.5	0.511 ± 0.009	0.506	0.183 ± 0.004	0.181	0.077 ± 0.001	0.077	0.054 ± 0.001	0.054
	0.6	0.543 ± 0.009	0.537	0.186 ± 0.004	0.185	0.077 ± 0.001	0.076	0.052 ± 0.001	0.054
HWC-P	0.4	0.346 ± 0.007	0.340	0.164 ± 0.004	0.163	0.078 ± 0.001	0.077	0.052 ± 0.001	0.055
	0.5	0.347 ± 0.007	0.341	0.164 ± 0.004	0.163	0.077 ± 0.001	0.077	0.053 ± 0.001	0.055
	0.6	0.344 ± 0.008	0.337	0.164 ± 0.005	0.162	0.077 ± 0.001	0.077	0.053 ± 0.001	0.055

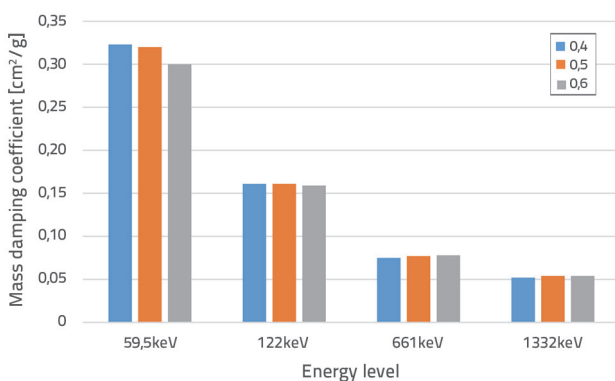


Figure 13. Mass absorption coefficients of CCs at different w/c ratios

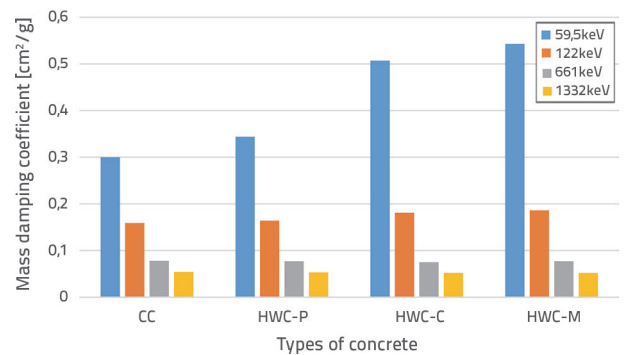


Figure 14. Mass attenuation coefficients of CCs (0.60 cement/c ratio), HWC-P, HWC, HWC-C, and HWC-M for different energy levels

Sharifi et al. [6] calculated the mass absorption coefficients in the range of 0.0788 to 0.056 and 0.0781 to 0.052 cm<sup>2</sup>/g for energy levels of 661 and 1,332 keV, respectively, and in CC with densities

of 3.35 and 2.33 g/cm<sup>3</sup>, respectively. Shams et al. [7] found that the mass attenuation coefficient at 1,332 keV of concretes with 100 % barite and hematite aggregates with densities of 3,061 and

3,007 g/cm<sup>3</sup>, respectively, were equal to 0.043 cm<sup>2</sup>/g. Researchers studying the mass attenuation coefficients of barite, hematite, and magnetite aggregate concretes showed that concrete produced using these aggregates can improve the radiation absorption properties of the concrete [4, 6, 7]. In this study, heavy concretes produced with pyrite, chromium, and magnetite aggregates absorb more X-rays than CCs. The heavy concrete mass absorption in this study is in agreement with related studies in the literature [4, 6, 7, 21]. As seen in Figure 14, the mass attenuation coefficients of CCs and HWCs are equal at 661 and 1332 keV. Yılmaz et al. [27] found the theoretical mass attenuation coefficient of 0.078 cm<sup>2</sup>/g at a 661 keV energy level in mortar samples with a density between 1.89 and 2.09 g/cm<sup>3</sup>. At high energy levels, although the density of the concrete is different, the mass attenuation coefficients approach each other and even take the same value. In concretes with the lowest hardened concrete density of 2,282 g/cm<sup>3</sup> and the highest magnetite aggregate hardened concrete density of 3,01 g/cm<sup>3</sup>, the mass attenuation coefficients of concretes at 661 and 1332 keV energy levels are equal. By keeping the water amount constant in HWC, concretes with a high cement/c ratio that can absorb more X-rays are produced. Concrete density is an important factor in the absorption of radiation; concrete with lower strength with increased radiation absorption capabilities can be produced. Figure 14 shows the experimentally measured mass absorption coefficients of CCs with a w/c ratio of 0.6 and heavy concretes with pyrite, chromium, and magnetite aggregates at energy levels of 59.5, 122, 661, and 1332 keV. The results show that the absorption coefficient decreases with increasing energy. In addition, no increasing or decreasing relationship was observed in the absorption coefficient due to the increasing w/c ratio change. Table 6 shows the density of 2,282 g/cm<sup>3</sup> at 59.5 keV energy level 0.3 cm<sup>2</sup>/g, at 1332 keV energy level 0.054 cm<sup>2</sup>/g CC with 3.01 g/cm<sup>3</sup> density at 59.5 keV energy level 0.543 cm<sup>2</sup>/g. The concrete thickness required to reduce the energy level of heavy concrete from 1,332 to 0.01 keV is at least 12.69 and 5.32 cm for CC and HWC-M, respectively, with 0.054 cm<sup>2</sup>/g magnetite aggregate at 59.5 keV energy level. Using heavy concrete instead of CC at 59.5 keV provides a reduction of 41.92 % in unit concrete volume. To reduce the energy level from 1,332 to 0.01 keV, concrete thicknesses of 95.93 and 72.59 cm are required for CC and HWC-M, respectively. At 1,332 keV, a reduction of 24.33 % was achieved in the unit concrete volume compared to CC. Considering that heavy aggregate used in concrete is more difficult to procure and process in crushing plants, heavy aggregates will increase the cost of concrete. In this respect, the use of CC at high energies may provide an advantage over HWC.

## 4. Conclusion

The key conclusions are given as follows:

- Pyrite, chromium, and magnetite minerals can be used in the production of HWCs. Heavy concrete with the targeted slump and strength class can be produced with aggregates containing chromium, pyrite, and magnetite.
- Increasing the w/c ratio by decreasing the amount of cement, reduced the unit volume weight in concretes with a lower specific gravity aggregate than cement. Aggregates with a specific weight higher than cement increased the density of concrete.
- In concretes with the similar w/c ratios, the use of aggregates with different specific weights had no impact on the concrete's elastic modulus. Compressive strength is the main determining factor on the modulus of elasticity of normal weight and heavy concretes.
- Concretes with higher densities were better at absorbing more radiation. The compressive strength of HWCs decreased with increasing w/c ratios (amount of water kept constant). However, the density increased due to the replacement of aggregate, which has a higher density than cement. This situation increased the radiation absorption property of low-strength, high-density concretes.
- In the study, there is no relation between concrete's strength and its radiation absorption. High concrete strength does not correlate to the high radiation mass attenuation coefficient of concrete.
- With increasing energy levels, the mass attenuation coefficient of the materials decreased. Equal mass attenuation coefficients were measured in CC and HWCs. The use of HWC in absorbing low-energy radiation provided more benefits than CC. The difference in thickness, which is the advantage of HWC, in absorbing high-energy radiation was reduced.
- With increasing unit weight, the attenuation coefficient increased. For the concretes produced in the study, the highest radiation attenuation coefficient was obtained for concretes produced with magnetite aggregate.

## Acknowledgment

This work was supported by the Coordinator of the Scientific Research Projects of Recep Tayyip Erdoğan University (RTEU-BAP, Project No: 2015.53001.109.03.02) in 2015.

## REFERENCES

- [1] Akyuz, S.: Heavy Concrete with Barite Aggregate for Protection from Gamma Rays, *İTÜ Journal*, (1977) 5, pp. 59-69
- [2] Saidani K., Ajam, L., Ouezdou, M.B.: Barite powder as sand substitution in concrete: Effect on some mechanical properties, *Construction and Building Materials*, 95 (2015), pp 287-295, doi: 10.1016/j.conbuildmat.2015.07.140
- [3] Ozen, S., Sengul, C., Erenoğlu, T., Çolak, U., Reyhancan, I.A. ve Taşdemir, M.A.: Properties of Heavyweight Concrete for Structural and Radiation Shielding Purposes, *Arab Journal Science Engineering*, (2016) 41, pp. 1573-1584
- [4] Otto, B., Gur, A., Kavaz, E., Cakir, T., Yaltay, N.: Determination of gamma and fast neutron shielding parameters of magnetite concretes, *Progress in Nuclear Energy*, (2016) 92, pp. 71-80, <https://doi.org/10.1016/j.pnucene.2016.06.011>
- [5] TS EN 206, 2017. Concrete- Feature, manufacturing and suitability. Turkish Standard, Ankara.
- [6] Sharifi, Sh., Bagheri, R., Shirmard, S.P.: Comparison of shielding properties for ordinary, barite, serpentine and steel-magnetite concretes using MCNP-4C code and available experimental results, *Annals of Nuclear Energy*, (2013) 53, pp. 529-534, <https://doi.org/10.1016/j.anucene.2012.09.015>
- [7] Shams, T., Eftekhari, M., Shirani, A.: Investigation of gamma radiation attenuation in heavy concrete shields containing hematite and barite aggregates in multi-layered and mixed forms, *Construction and Building Materials*, 182 (2018), pp.35-42, <https://doi.org/10.1016/j.conbuildmat.2018.06.032>
- [8] Quda, A.: Development of high-performance heavy density concrete using different aggregates for gamma-ray shielding, *Progress in Nuclear Energy*, (2015) 79, pp. 48-55, <https://doi.org/10.1016/j.pnucene.2014.11.009>
- [9] Waly, E.S.A., Bourham, M.A.: Comparative study of different concrete composition as gamma-ray shielding materials, *Annals of Nuclear Energy*, (2015) 85, pp. 306-310, <https://doi.org/10.1016/j.anucene.2015.05.011>
- [10] Ogawa, T., Morev, M.N., Limoto, T., Kosako, T.: Measurements of activation reaction rates in transverse shielding concrete exposed to the secondary particle field produced by intermediate energy heavy ions on an iron target, *Nuclear Instruments and Methods in Physics Research B*, 271 (2012), pp. 65-71, <https://doi.org/10.1016/j.nimb.2011.11.008>
- [11] Kilincarslan, S., Akkurt, I., Basyigit, C.: The effect of barite rate on some physical and mechanical properties of concretes. *Materials Science and Engineering*, (2006) A 424, pp. 83-86, <https://doi.org/10.1016/j.msea.2006.02.033>
- [12] Lotfi-Omran, O., Sadrmomtazi, A., Nikbin, I.M.: A comprehensive study on the effect of water to cement ratio on the mechanical and radiation shielding properties of heavyweight concrete, *Construction and Building Materials*, 229 (2019), pp. 116905, <https://doi.org/10.1016/j.conbuildmat.2019.116905>
- [13] Topcu, I.B.: Concrete Technology. Eskişehir.2006
- [14] Prochon, P., Piotrowski, T.: The effect of cement and aggregate type and w/c ratio on the bound water content and neutron shielding efficiency of concretes, *Construction and Building Materials*, 264 (2020), 120210. <https://doi.org/10.1016/j.conbuildmat.2020.120210>
- [15] Bellum, R.R., Muniraj, K., Madduru, S.R.C.: Investigation on modulus of elasticity of fly ash-ground granulated blast furnace slag blended geopolymer concrete, *Materials Today: Proceedings*, 27 (2020), pp. 718-723, <https://doi.org/10.1016/j.matpr.2019.11.299>
- [16] Topçu, I.B., Bilir, T., Boga, A.R.: Estimation of the modulus of elasticity of slag concrete by using composite material models, *Construction and Building Materials*, 24 (2010), pp. 741-748, <https://doi.org/10.1016/j.conbuildmat.2009.10.034>
- [17] Yıldırım, H., Sengul, O.: Modulus of elasticity of substandard and normal concretes, *Construction and Building Materials*, 25 (2011), pp. 1645-1652, <https://doi.org/10.1016/j.conbuildmat.2010.10.009>
- [18] Briševac, Z., Hrženjak, P., Buljan, R.: Models for estimating uniaxial compressive strength and elastic modulus, *GRAĐEVINAR*, 68 (2016) 1, pp. 19-28, <https://doi.org/10.14256/JCE.1431.2015>
- [19] Matulić, P., Juradin, S., Marušić, E., Domazet, A.: Effect of test specimen size on mechanical properties of shotcrete, *GRAĐEVINAR*, 68 (2016) 4, pp. 301-309, <https://doi.org/10.14256/JCE.1240.2014>
- [20] Vorobjovas, V., Vaitkus, A.: Use of local aggregates in high modulus asphalt concrete layers, *GRAĐEVINAR*, 65 (2013) 4, pp. 353-360, <https://doi.org/10.14256/JCE.886.2013>
- [21] Neira, P., Bennun, L., Pradena, M., Gómez, J.: Prediction of concrete compressive strength through artificial neural networks, *GRAĐEVINAR*, 72 (2020) 7, pp. 585-592, <https://doi.org/10.14256/JCE.2438.2018>
- [22] Hussain, R.R., Shuraim, A.B., Aslam, F., Alhozaimy, A.M.A., Al-Humaiqani, M.M.: Coupled effect of coarse aggregate and micro-silica on the relation between strength and elasticity of high performance concrete, *Construction and Building Materials*, 175 (2018), pp. 321-332, <https://doi.org/10.1016/j.conbuildmat.2018.04.192>
- [23] Torić, N., Boko, I., Peroš, B.: Degradation of mechanical properties of high-strength concrete after exposure to fire, *GRAĐEVINAR*, 63 (2011) 12, pp. 1033-1041.
- [24] Barišić, I., Dimter, S., Rukavina, T.: Cement stabilizations - characterization of materials and design criteria, *GRAĐEVINAR*, 63 (2011) 2, pp. 135-142.
- [25] Bilir, T.: Investigation of performances of some empirical and composite models for predicting the modulus of elasticity of high strength concretes incorporating ground pumice and silica fume, *Construction and Building Materials*, 127 (2016), pp. 850-860.
- [26] Baltas, H., Sirin, M., Celik, A., Ustabas, İ, El-Khayatt, A.M.: Radiation shielding properties of mortars with minerals and ores additives, *Cement and Concrete Composites* (2019), 97 (2016), pp. 268-278, <https://doi.org/10.1016/j.cemconcomp.2019.01.006>
- [27] Yılmaz, E., Baltas, H., Kiris, E., Ustabas, İ, Cevik, U., ve El-Khayatt, A.M.: Gamma ray and neutron shielding properties of some concrete materials. *Annals of Nuclear Energy*, 38 (2011), pp. 204-212, <https://doi.org/10.1016/j.anucene.2011.06.011>
- [28] Yetim, M.: Investigation of the Effects of Sanliurfa Lime Powder on Physical and Mechanical Properties of Concrete by Cement Substitution. Sanliurfa, Turkey: Harran University Institute of Science and Technology, 2021.